Effects of Control Power and Guidance Cues on Lunar Lander Handling Qualities

Karl D. Bilimoria[*]
NASA Ames Research Center, Moffett Field, CA 94035

A piloted simulation was conducted to assess handling qualities for a precision lunar landing task from terminal descent to touchdown. The experiment variables were control power and guidance cues. A dynamics and control model was derived from Apollo Lunar Module data, and guidance laws were designed to follow a reference trajectory. The experiment was conducted on the large motion base Vertical Motion Simulator at the NASA Ames Research Center. Six pilot astronauts served as evaluation pilots, providing Cooper-Harper ratings, Task Load Index ratings, and qualitative comments. The piloting task was to fly a final approach profile from 500 ft altitude to touchdown, starting from a 250 ft lateral offset to the landing site. Following guidance cues, the pilots were able to accomplish this task for control powers ranging from 100% to 15% of the nominal (Apollo) value. The handling qualities were satisfactory (Level 1) at nominal control power, and degraded as control power decreased. Without guidance cues, in the limited time available for this experiment, the evaluation pilots were unable to develop a flying technique for the precision landing task with lateral offset approach. This highlights the need for guidance cues in future lunar operations that may require precision landing capability.

Introduction

Handling qualities are those characteristics of a flight vehicle that govern the ease and precision with which a pilot is able to perform a flying task.[1] They are a manifestation of the interaction between various factors that influence pilot perception of how well (or poorly) a vehicle can be used to accomplish a desired mission. These factors include the stability and control characteristics of the bare vehicle, the control systems that enhance these characteristics, the inceptors (e.g., control column or throttle lever) used by the pilot to transmit control commands, the visual cues from cockpit windows and displays/instrumentation that provide flight information to the pilot, and other cues (e.g., aural, tactile) that assist the pilot in the execution of the flying task.

The handling qualities of aircraft have been studied for quite some time.[2–4] Reference standards for the handling qualities of both fixed-wing aircraft[5] and rotary-wing aircraft[6] have been developed, and are now in common use. Broadly speaking, these standards define a subset of the dynamics/control design space that provides good handling qualities for a given vehicle type and flying task. For example, the standards may specify a range of combinations of damping and natural frequency for a large aircraft during landing.

At this time, no reference standards exist for handling qualities of piloted spacecraft. Handling qualities have been assessed, at least at a basic level, for some space vehicles.[7–10] However, the focus of these studies was to evaluate or address deficiencies in the handling qualities of a specific vehicle, rather than to map out handling qualities variations over a broad range of many design variables to determine desirable regions in the design space for a class of vehicles.

A new generation of piloted spacecraft is now being designed.[11] The ability of pilots to successfully carry out their missions will be determined in part by the handling qualities of these new spacecraft. Some operational tasks may be fully automated, while other tasks are executed with a human pilot fully engaged in the control loop. Even for the nominally automated tasks, there must always be the capability for a human pilot to take control at a relatively basic level – whether due to failure of an automated system, or of some component of the spacecraft. In these cases of emergency reversion to manual control, where the pilot role abruptly switches from monitoring to active control, it is even more important that the vehicle have good handling qualities. It is therefore desirable for spacecraft designers to assess early in the design cycle what the handling qualities will likely be, and to adjust their

---

[*] Research Scientist, Automation Concepts Branch; Mail Stop 210-10; *Karl.Bilimoria@nasa.gov*. Associate Fellow, AIAA.

design if necessary to ensure that adequate handling qualities are preserved even in degraded or failed operational modes.

An effort to develop design guidelines for spacecraft handling qualities was initiated by NASA in 2007. A comprehensive set of guidelines should cover all classes of spacecraft and phases of flight; however, near-term NASA program goals make it necessary to focus initially on a few specific and relevant aspects. References 12 and 13 describe two recent experiments investigating the handling qualities of spacecraft docking in low Earth orbit.

This paper reports an experiment investigating the terminal descent to touchdown phase of lunar landing, which is a particularly challenging flying task. In an interview,[14] Neil Armstrong said: "The most difficult part from my perspective, and the one that gave me the most pause, was the final descent to landing. That was far and away the most complex part of the flight. … I thought that the lunar descent on a ten scale was probably a thirteen."

In the Apollo lunar missions, it was sufficient to land within several hundred feet of the designated landing site. Future lunar base operations may require precision landing capability at designated sites due to lunar dust issues. This work investigates the handling qualities for a precision lunar landing task from terminal descent to touchdown, for various control powers, with and without guidance cues. The following section describes the experiment design. The next section presents the dynamics/control model derived from Apollo Lunar Lander data as well as the precision landing guidance laws developed for this work; it is followed by a section describing the high-fidelity simulation environment. Results from a piloted high-fidelity-motion simulation are then presented, followed by conclusions.

Experiment Design

A piloted evaluation of lunar lander handling qualities was conducted in May–June 2007 on the NASA Ames Vertical Motion Simulator (VMS). This section describes various aspects of the experiment design.

Flying Task

This experiment evaluated handling qualities for a precision landing task. Coarse trajectory changes were made by firing opposing Reaction Control System (RCS) jets to change the attitude of the lander and hence tilt the thrust vector of the descent engine. In a near-level attitude, fine trajectory changes could be made by firing RCS jets in the same direction. Feedback guidance laws were developed for flying the precision landing task, and the corresponding guidance cues were displayed to the pilot via cockpit instrumentation. Details of the dynamics and control model are presented in the next section.
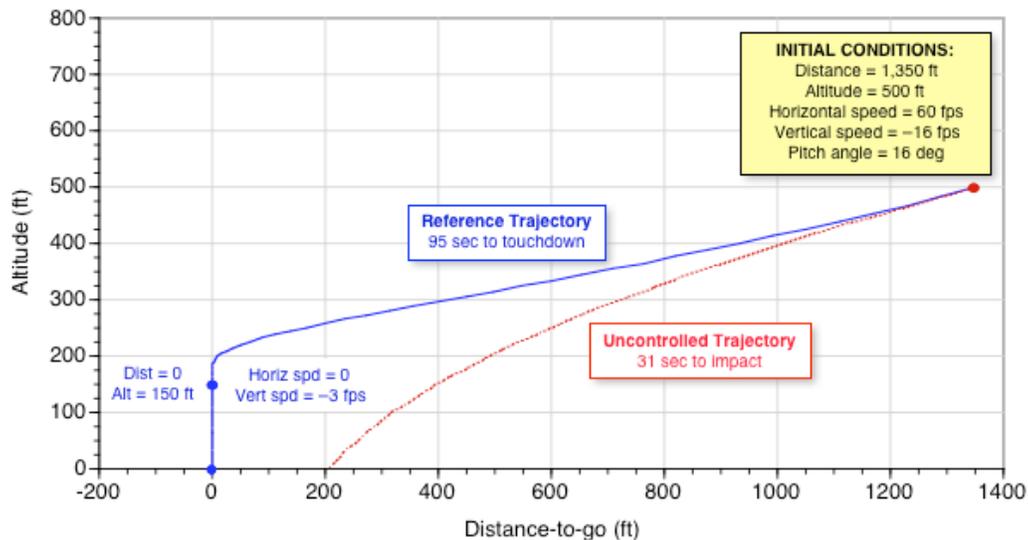
Figure 1. Reference trajectory profile in the vertical plane

The task began at 500 ft (152.4 m) altitude with a forward speed of 60 fps (18.3 m/s) and a descent rate of 16 fps (4.9 m/s); for Apollo missions this was known as "low gate" and represented the point on the trajectory where the manual flying phase would begin. At this point, the spacecraft was at 1,350 ft (411.5 m) range from the designated

touchdown point. The desired trajectory brought the spacecraft directly above the touchdown point at an altitude of 150 ft (45.7 m) with a descent rate of 3 fps (0.9 m/s). This rate of descent was held constant until one of the 6 ft (1.8 m) probes attached to the lander legs made contact with the lunar surface. A shut-off command was then sent to the main engine, and the vehicle dropped until the legs settled on the lunar surface. This reference trajectory profile is illustrated in Fig. 1. For comparison, it also shows the uncontrolled trajectory that would result if no pilot inputs were made starting from an initial condition with vertical force equilibrium.

The dynamics of the trajectory described above are confined to the vertical plane. In order to excite the lateral dynamics, the initial condition was given a lateral offset of 250 ft (76.2 m) from the touchdown point. This means that the initial velocity vector did not point directly at the landing site.

Test Matrix

The objective of this experiment was to evaluate the effects of control power and guidance cues on handling qualities for a precision lunar landing task. Control power refers to the RCS jet thrust, which directly affects angular acceleration for opposing jet firings and translational acceleration for same-direction firings. Six values of control power ranging from 100% to 15% of the nominal Apollo Lunar Module value were selected for evaluation based on trial runs with development pilots prior to the experiment. The primary goal of the experiment was to assess the variation of handling qualities with control power. A secondary experiment goal was to assess handling qualities with and without guidance cues. The test matrix is depicted in Table 1.

Table 1. Experiment matrix

Control Power → Guidance ↓	0.15X	0.2X	0.25X	0.3X	0.5X	1X (Baseline)
ON						
OFF						

The original experiment plan was to conduct handling qualities assessments for a lateral offset approach with guidance on and off. However, it was found that the precision landing task with offset approach and guidance off was extremely difficult, and the pilots were unable to develop a flying technique for this task in the limited time available. A centerline approach (zero lateral offset) was flyable with guidance off, and was therefore substituted in the test matrix. It should be noted that a direct comparison of guidance on/off cases cannot be made now, since the flying tasks are quite different.

Evaluation Pilots

Six active-duty pilot astronauts from the NASA Johnson Space Center served as evaluation pilots. All were male and had substantial training/experience as test pilots prior to astronaut selection. They had logged an average of about 5,000 hours on various types of aircraft, and each had received many years of pilot astronaut training. Each pilot was available to the experimenters for about 8 hours, and this time constraint was incorporated into the experiment design.

Training Procedures

Upon arrival, the pilot received a detailed briefing on the experiment background and objectives, flying task, control system, test matrix, and data collection procedures. Including discussion time, this session lasted approximately one hour. This was followed by a one-hour training and familiarization session in the simulator cockpit, where the pilot practiced the flying task for various control powers with guidance on as well as off, until he felt comfortable that most of the learning curve was behind him.

Data Collection Procedures

Each pilot encountered the six control powers in a randomized sequence and was not told the value of the control power. Pilots first flew all configurations for offset approach with guidance on, and then flew all configurations for

centerline approach with guidance off. For each test configuration (e.g., offset approach with guidance on and 100% control power), the pilot flew three data collection runs.

In handling qualities experiments, pilots are generally asked to make a composite assessment of the overall performance across all data collection runs for a test configuration. It is important to note that this assessment takes into account not just the quantitative evaluation of the end-point (e.g., touchdown) performance but also a qualitative evaluation of the manner in which the vehicle gets to the end-point. This overall assessment of desired, adequate, or inadequate performance is utilized for walking through the decision tree in the Cooper-Harper chart.[1] Desired performance is necessary (but not sufficient) for Level 1 ratings, and adequate performance is necessary (but not sufficient) for Level 2 ratings.

At the end of each run, relevant touchdown performance parameters (see Table 2) were displayed to the pilot and experimenter; values outside the adequate performance bounds were colored red. The values of adequate performance bounds for key parameters were obtained from a survey of Apollo Lunar Module literature; the 15 ft (4.6 m) range for this precision landing task was obtained as half of the diagonal distance between the lander legs. It is noted that there were no specified values for desired performance bounds. These values should ideally be determined by working with development pilots before the experiment, but are sometimes specified simply as a fraction (e.g., half) of the adequate values. In this experiment, the evaluation pilots were asked to make their own assessment of desired touchdown performance.

Table 2. Limits of adequate touchdown performance

Limits of Touchdown Values	
Roll Angle ± 6 deg	Roll Rate ± 6 deg/sec
Pitch Angle ± 6 deg	Pitch Rate ± 6 deg/sec
Range 15 ft = 4.6 m	Yaw Rate ± 1.5 deg/sec
Horizontal Speed 4 fps = 1.2 m/s	Descent Rate 8 fps = 2.4 m/s
Descent Engine Propellant Burn 1,500 lbm = 680 kg	RCS Jets Propellant Burn 150 lbm = 68 kg

After making a composite assessment of the overall performance across the three data collection runs for a test configuration, pilots walked through the Cooper-Harper chart and assigned a handling qualities rating for that test configuration. Next, they assigned ratings for each of the six components of the NASA Task Load Index.[15] These six components were: physical demand, mental demand, temporal demand, performance, effort, and frustration. As appropriate, pilots also made qualitative comments about the test configuration they had just evaluated. All pilot comments were recorded on electronic media; the experimenter noted key points.

After all test configurations had been evaluated, there was a debrief session. The pilots were asked to fill out a one-page questionnaire designed to elicit high-level comments on cockpit displays, out-the-window displays, guidance cues, control response, and experiment design. This was followed by a discussion with the experimenter.

Dynamics and Control Model of Lunar Lander

Since NASA's Constellation program lunar lander[16] (currently named Altair) was still in the configuration design stage when this study was initiated in January 2007, a generic model was created based on Apollo Lunar Module data gathered from various sources such as Ref. 17. In the model used for this work, the lunar lander body axes system was a conventional aircraft-like system with origin at the center-of-mass (c.m.); see schematic in Fig. 2.

Vehicle Mass/Inertia Model

The initial mass of the vehicle is 543 slugs (7,925 kg); it then varies due to consumption of propellant by the descent engine and RCS jets. Vehicle moments of inertia are given by:

$I_{xx} = 16,099$ slug-ft^2; $I_{yy} = 13,629$ slug-ft^2; $I_{zz} = 12,750$ slug-ft^2;

$I_{xz} = -652$ slug-ft^2; I_{xy} and I_{yz} taken to be zero.

During the terminal descent to touchdown phase the vehicle mass decreases by only 5% due to propellant consumption. Hence in this model it is assumed that moments of inertia are constant and that the vehicle c.m. location remains constant.
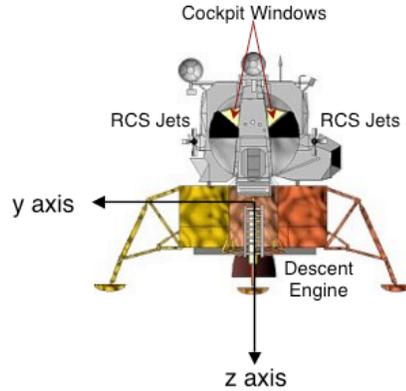
Figure 2. Schematic of Apollo Lunar Module

Descent Engine

The descent engine is the spacecraft's main rocket engine, with a specific impulse of 311 sec. For the landing task, it is used to regulate the descent rate and for coarse trajectory control in the horizontal plane by rolling and/or pitching the vehicle. In this model, the engine does not gimbal and the thrust line passes through the vehicle center of mass. Propellant mass budgeted for the nominal landing profile, including reserves, is 50 slugs (730 kg).

The maximum thrust is 10,000 lb (44,482 N), and it can be controlled by a throttle between 10% and 60% of the maximum value, directed along the negative body z-axis. The thrust command, T_{cmd}, consists of two parts. The primary part, T_{cmd}^*, is automatically computed as the force whose vertical component balances the vehicle's lunar weight in response to vehicle roll (ϕ) and pitch (θ) angles.

$$T_{cmd}^* = \frac{m \, g_{lunar}}{\cos\phi \, \cos\theta} \tag{1}$$

The secondary part of the thrust command, ΔT_{cmd}, is an increment derived from pilot input. There are two modes for pilot input: a throttle increment mode and a rate-of-descent mode. In the throttle increment mode, each inceptor "click" input by the pilot increments the thrust by ±1% of the upper throttle limit value of 6,000 lb. In the rate-of-descent mode, each inceptor "click" increments the commanded rate-of-descent rate by ±1 fps (0.3 m/s); the descent rate is regulated within a dead-band of ±0.1 fps (0.03 m/s) by a proportional feedback controller with a time constant $\tau = 1.5$ sec.

$$\Delta T_{cmd}^{ROD} = \frac{m}{\cos\phi \, \cos\theta} \left(\frac{\dot{h}_{cmd} - \dot{h}}{\tau} \right) \tag{2}$$

Engine response to thrust commands is modeled as a first-order system, with a time constant of 0.11 sec. Hence the actual thrust produced by the descent engine, T, lags the commanded thrust $T_{cmd} = T_{cmd}^* + \Delta T_{cmd}$.

Reaction Control System Jets

There are four clusters, each of which has four RCS jets with thrust axes along the vehicle body axes. There are a total of 16 jets aligned as follows: four jets each along ±z, two jets each along ±y, and two jets each along ±x. The RCS jet clusters are located at the corners of a square of length $2\ell = 11$ ft (3.4 m), located $\ell = 5.5$ ft (1.7 m) above the vehicle c.m. The nominal thrust of each jet, F^*, is 100 lb (445 N), with a specific impulse of 290 sec. The RCS

jets cannot be throttled, and have fast response dynamics on the order of 10 milliseconds. In this model, the response to an on/off command input is assumed instantaneous. Propellant mass budgeted for the nominal landing profile, including reserves, is 5 slugs (73 kg).

For the landing task, RCS jets are used for attitude control and for fine control of the trajectory in the horizontal plane when the vehicle is in a near-level attitude. For vehicle rotation commands, two jets are fired in opposition for roll/pitch/yaw commands to create a moment $2\,\mathcal{m}^* = 2\,\ell\,F^* = 1,100$ ft-lb (1,491 N-m), and there is no net force created. For vehicle translation commands, two jets are fired in the same direction to create a force $2\,F^* = 200$ lb (890 N) along the body x-axis and/or y-axis; note that these force(s) will generate pitch and/or roll moments due to the moment arm along the body z-axis. In this model, we are using aggregated forces/moments generated by the firing of various RCS jet combinations, i.e., selection and firing of individual jets are not modeled. It is noted that during the powered descent phases of flight, RCS jets are not used to create translation-only forces along the z-axis.

Direct translation control

Pilot inputs are made with a three-axis translation hand controller (THC); this control inceptor is used for fine control of the trajectory along the x and y body axes when the vehicle is in a near-level attitude. The control response type is acceleration command; this means that the appropriate RCS jets fire continuously to produce a constant force/acceleration for as long as the pilot holds the inceptor out of detent. For example, moving the THC forward will create a force of $2\,F^*$ (and hence an acceleration of $2\,F^*/m$) along the body x axis. Note that this will also create a nose-down pitching moment.

Attitude control

By tilting the descent engine thrust vector, attitude control provides indirect translation control for coarse trajectory changes. Pilot inputs are made with a three-axis rotation hand controller (RHC); this control inceptor is used for attitude stabilization/control along all three body axes. The control response type is Rate Command Attitude Hold (RCAH), implemented as described below.

Rate Command mode

This mode is in effect along all three axes when the inceptor is out of detent in any axis. It is also in effect when the inceptor is in detent along all three axes and the sum of the absolute values of roll, pitch, and yaw rates is not less than 2 deg/sec. The angular rate command is proportional to the inceptor displacement with a value of 20 deg/sec at full inceptor deflection. Error signals are generated as the difference between the actual and desired angular rates:

$$\begin{Bmatrix} p_{err} \\ q_{err} \\ r_{err} \end{Bmatrix} = \begin{Bmatrix} p - p_{cmd} \\ q - q_{cmd} \\ r - r_{cmd} \end{Bmatrix} \tag{3}$$

where p, q, r, are the roll, pitch, and yaw rates respectively along the vehicle body axes.

By firing RCS jets, control moments are generated about the appropriate axes until the error signals are driven to zero within a rate dead-band of 0.4 deg/sec.

Attitude Hold mode

This mode is in effect simultaneously along all three axes when the inceptor is in detent in all three axes, and the sum of the absolute values of roll, pitch, and yaw rates is less than 2 deg/sec. Error signals are given by:

$$\begin{Bmatrix} p_{err} \\ q_{err} \\ r_{err} \end{Bmatrix} = \begin{Bmatrix} p \\ q \\ r \end{Bmatrix}; \qquad \begin{Bmatrix} \phi_{err} \\ \theta_{err} \\ \psi_{err} \end{Bmatrix} = \begin{bmatrix} 1 & 0 & -\sin\theta \\ 0 & \cos\phi & \sin\phi\,\cos\theta \\ 0 & -\sin\phi & \cos\phi\,\cos\theta \end{bmatrix} \begin{Bmatrix} \phi - \phi_{hold} \\ \theta - \theta_{hold} \\ \psi - \psi_{hold} \end{Bmatrix} \tag{4}$$

where (ϕ, θ, ψ) are the current values of the vehicle Euler angles, and ($\phi_{hold}, \theta_{hold}, \psi_{hold}$) are the Euler angle values trapped when Attitude Hold mode was last entered.

American Institute of Aeronautics and Astronautics

By firing RCS jets, control moments are generated about the appropriate axes in accordance with the phase-plane relationship between error signals, as illustrated in Fig. 3 for the pitch axis. The blue switching curves depict the equality:

$$\theta_{err} = \pm \left[\left(\frac{1}{2\alpha_P} \right) (q_{err})^2 - \theta_{DB} \right] \tag{5a}$$

where α_P is the nominal pitch acceleration, approximated by $(2\mathcal{M}^* / I_{yy}) = 4.5$ deg/sec^2, and $\theta_{DB} = 0.3$ deg is the dead-band for pitch attitude error. The red switching curves depict the equality:

$$\theta_{err} = \pm \left[\left(\frac{1}{2k\alpha_P} \right) (q_{err})^2 + \theta_{DB} \right] \tag{5b}$$

where $k = 0.25$ denotes a parameter that represents a trade-off between RCS jets propellant consumption and error settling time.
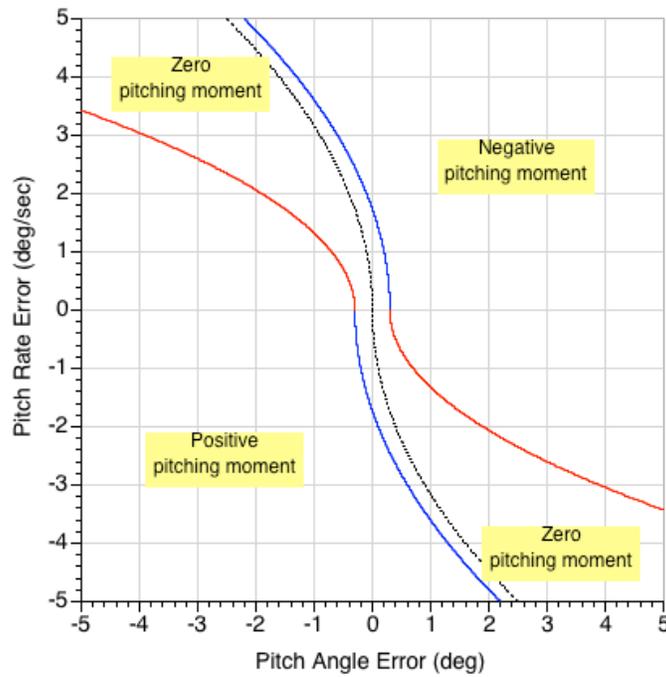
Figure 3. Switching curves with dead-bands (dotted curve is for exact time-optimal switching)

Similar phase-plane relationships are defined for the roll and yaw axes, except for a small difference in the value of the nominal acceleration α in Eqs. (5a,b); specifically, 4 deg/sec^2 for roll and 5 deg/sec^2 for yaw.

Guidance Laws

The Apollo lunar missions did not have a requirement for precision landing; it was sufficient to land within several hundred feet of the designated landing site. Therefore, the Apollo Lunar Module did not require, nor did it have, any active guidance cues displayed to the pilot. The guidance laws presented below were independently derived, and constitute one of the original contributions of this work. These laws were designed to follow a reference trajectory (see Fig. 1) from terminal descent to lunar touchdown. In the equations presented below, time is in units of seconds, distance is in units of feet, and speed is in units of feet per second. Variables along the reference trajectory are denoted by an asterisk superscript.

In the vertical dimension of the reference trajectory, the descent rate decreases linearly from 16 fps at 500 ft altitude to 3 fps at 150 ft altitude, and then remains constant at 3 fps as the altitude decreases to zero. Hence:

$$\dot{h}^* = (-0.03714\, h^* + 2.57)\ \text{ for }\ h^* \geq 150 \tag{6a}$$

$$\dot{h}^* = -3\ \text{ for }\ h^* < 150 \tag{6b}$$

Noting that $h^*(0) = 500$ ft, and analytically integrating Eq. (6a), we get:

$$h^*(t) = 430.8\,\exp(-0.03714\,t) + 69.2\ \text{ for }\ h^* \geq 150 \tag{7}$$

Let Δt^* denote the time interval for the vehicle to descend along the reference trajectory from some altitude h^* to 150 ft altitude. From Eq. (6a), we get

$$\Delta t^* = 26.93\ln\left(\frac{h^* - 69.2}{80.8}\right) \tag{8}$$

In the horizontal dimension of the reference trajectory, the horizontal speed, V_{horiz}, at range R from the landing site decreases to zero speed at zero range. Note that this needs to happen in the time Δt^* that it takes for the vehicle to descend to 150 ft altitude along the vertical dimension of the reference trajectory. The horizontal acceleration varies along the reference trajectory. However, for analytical convenience, let a_{horiz} represent an equivalent average acceleration in the horizontal plane over the time interval Δt. From kinematics, we have $a_{horiz} = -V_{horiz}/\Delta t^*$ and $R = V_{horiz}\,\Delta t^* + 0.5\,a_{horiz}\,(\Delta t^*)^2$; hence $V_{horiz} = 2\,R/\Delta t^*$. Noting that $\dot{R} = V_{horiz} = 2\,R/\Delta t^*$, and $R(0) = 1{,}350$ ft, we get:

$$R(t) = 1350\,\exp\left(\frac{-2}{\Delta t^*}\,t\right) \tag{9}$$

Substituting Eq. (8) into Eq. (9), and comparing the resultant equation with Eq. (7) yields:

$$h^* = 69.2 + \left(\frac{80.8^{\left(\ln\sqrt{R/1350}\,\right)}}{430.8}\right)^{\frac{1}{\left(\ln\sqrt{R/1350}\,\right)-1}} \tag{10}$$

The altitude rate along the reference trajectory is given by Eq. (6). For the general case where the vehicle is not on the reference trajectory, i.e., $h \neq h^*$, the vertical speed guidance law is of the form $\dot{h}^G = \dot{h}^* + K_h\,(h^* - h)$ where h is the actual altitude and $K_h > 0$ is a feedback gain. Hence:

$$\dot{h}^G = \left(-0.03714\, h^* + 2.57\right) + \left(\frac{h^* - h}{\tau}\right) \tag{11}$$

where $\tau = 1/K_h = 25$ sec and h^* is obtained from Eq. (10). $\dot{h}^G$ is set to a constant value of -3 fps when h first drops below 150 ft. To limit the effect of large altitude errors, the value of $\dot{h}^G$ obtained from Eq. (11) is bounded by 0 and -30 fps.

Substituting Eq. (8) into the equation $V_{horiz} = 2\,R/\Delta t^*$, and then substituting Eq. (10) into the resulting equation yields the following relationship along the reference trajectory:

$$V_{horiz}^* = 0.04444\,R\left(1 - 0.5\ln(R/1350)\right) \tag{12}$$

Let V_N^* and V_E^* denote the North and East components of the horizontal speed V_{horiz}, respectively, along the reference trajectory. Also, let x and y denote North and East components, respectively, of the vehicle's range from the landing site, i.e., $R = \sqrt{x^2 + y^2}$. Then:

$$V_N^* = 0.04444\, x \left(\ln \sqrt{R/1350} - 1 \right) \tag{13a}$$

$$V_E^* = 0.04444\, y \left(\ln \sqrt{R/1350} - 1 \right) \tag{13b}$$

For numerical conditioning, V_N^* and V_E^* are set to zero if $R < 0.1$ ft.

Transforming the above guidance velocity components from Moon-fixed axes to vehicle-body axes, and noting that the down velocity component $V_D = -\dot{h}$, yields:

$$V_X^G = (\cos\theta \cos\psi)\, V_N^G + (\cos\theta \sin\psi)\, V_E^G + (\sin\theta)\, \dot{h}^G \tag{14a}$$

$$V_Y^G = (\sin\phi \sin\theta \cos\psi - \cos\phi \sin\psi)\, V_N^G + (\sin\phi \sin\theta \sin\psi + \cos\phi \cos\psi)\, V_E^G - (\sin\phi \cos\theta)\, \dot{h}^G \tag{14b}$$

where V_X^G and V_Y^G are guidance velocity components along the vehicle body x and y axes, respectively.

The North and East components of acceleration along the reference trajectory can be determined from analytical differentiation of Eq. (13). For the general case where the vehicle is not on the reference trajectory, i.e., $V \neq V^G$, the acceleration guidance law has the form $a^G = a^* + K_V (V^* - V)$ where V is the actual velocity and $K_V > 0$ is a feedback gain. The North and East components of acceleration guidance are obtained as:

$$a_N^G = \left\{ \frac{V_N\, V_N^*}{x} + \left(\frac{0.02222\, x\, \dot{R}}{R} \right) \right\} + \left(\frac{V_N^* - V_N}{\tau} \right) \tag{15a}$$

$$a_E^G = \left\{ \frac{V_E\, V_E^*}{y} + \left(\frac{0.02222\, y\, \dot{R}}{R} \right) \right\} + \left(\frac{V_E^* - V_E}{\tau} \right) \tag{15b}$$

where $\tau = 1/K_V = 8$ sec. For numerical conditioning, a_N is set to zero if $|x|$ is less than 0.1 ft; a similar rule applies in the y dimension.

Noting that tilting the descent engine thrust force, T, creates an acceleration in the horizontal plane, we have:

$$m\, a_N = -T\, (\cos\phi \sin\theta \cos\psi + \sin\phi \sin\psi) \tag{16a}$$

$$m\, a_E = -T\, (\cos\phi \sin\theta \sin\psi - \sin\phi \cos\psi) \tag{16b}$$

The guidance roll and pitch angles, ϕ^G and θ^G, are determined from Eqs. (16a,b) as:

$$\phi^G = \sin^{-1}\left\{ \frac{-m}{T} \left(a_N^G \sin\psi - a_E^G \cos\psi \right) \right\} \tag{17a}$$

$$\theta^G = \sin^{-1}\left\{ \frac{-m}{T \cos\phi^G} \left(a_N^G \cos\psi + a_E^G \sin\psi \right) \right\} \tag{17b}$$

To limit the effect of large trajectory errors, the values of ϕ^G and θ^G are bounded by ±45 deg.

For guidance purposes, the range R is considered as the independent variable. First, the value of h^* is computed from Eq. (10) – this is the altitude at which the vehicle would be flying if it were on the reference trajectory at range R from the landing site. The altitude rate guidance can now be computed from Eq. (11). This enables computation

American Institute of Aeronautics and Astronautics

of the velocity components from Eqs. (13) and (14). Finally, the guidance roll and pitch angles can be computed from Eq. (17).

Guidance cues are presented to the pilot as errors from the desired vehicle states. These errors are computed as the differences between: the guidance roll/pitch angle given by Eq. (17) and the corresponding actual values, and the guidance velocity components along the vehicle body axes given by Eq. (14) and the corresponding actual values. Details on the display of these guidance cues are presented in the next section.

Simulation Environment

The experiment was conducted on the Vertical Motion Simulator (VMS) at NASA Ames Research Center. The VMS is a large motion base simulator[18] that has been used for numerous handling qualities evaluations.[19] The Apollo Lunar Lander pilot stations had a standing configuration to improve downward visibility and reduce vehicle mass by eliminating seats. The VMS cab was modified to provide a similar cockpit configuration; see Fig. 4. The evaluation pilot occupied the left station; the right station was occupied by the experimenter during training runs but was unoccupied for data collection runs. At each pilot station, there was a three-axis rotation hand controller (RHC) and a three-axis translation hand controller (THC) mounted on the right and left armrest, respectively. Twisting the THC toggled between the descent engine control modes of throttle increment and descent rate. Up/down motion of the THC adjusted the commanded value of the throttle increment or rate of descent, depending on the selected mode.
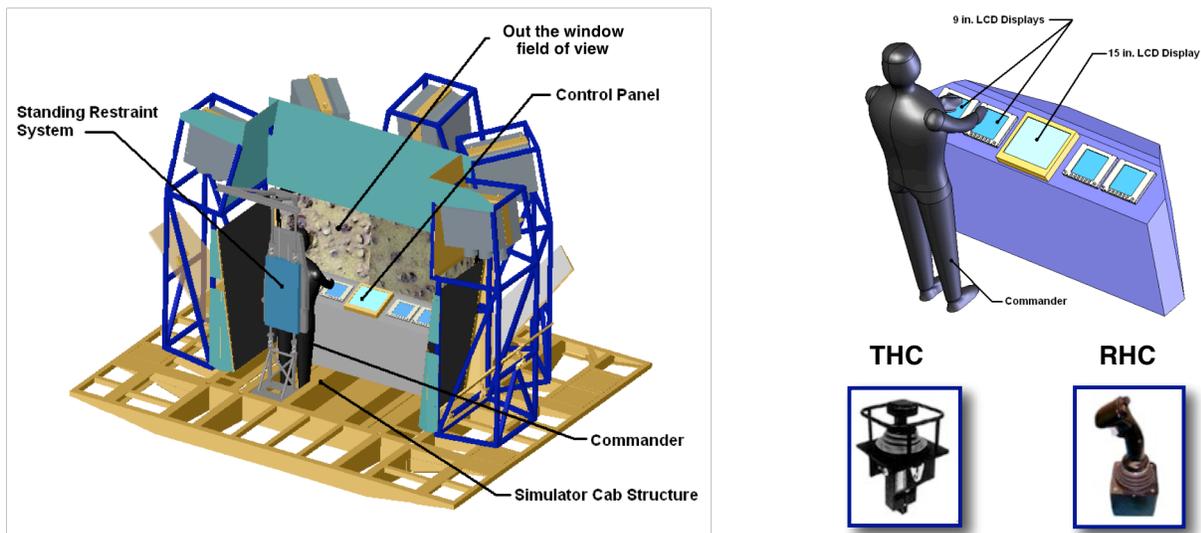
Figure 4. Simulator cockpit layout

Cockpit displays were mounted on a console with two 9-inch LCD monitors at each pilot station and a 15-inch LCD monitor in the center. The pilot station displays are shown in Fig. 5; the center monitor displayed color-coded touchdown performance parameters given in Table 2.

The right display shows an Attitude Direction Indicator (ADI) with a digital readout of the roll, pitch, and yaw angles. The green bars on the ADI are error needles that provide guidance for roll, pitch, and yaw angles using Eq. 17. This guidance is "fly to" which means that in the illustration of Fig. 5 the pilot should use the RHC to roll right, pitch down, and yaw right to drive the error needles to zero. In the experiment, the yaw guidance was turned off (yaw needle locked at zero), and pilots were advised not to make any yaw inputs because it added significant workload while adding little value to the flying task. For configurations with guidance off, all three needles were locked at zero. The small triangles on the scales around the ADI show the roll, pitch and yaw rates; each tick mark on the scale is 5 deg/sec. On the lower right of the ADI is an annunciator for the throttle mode (throttle increment or descent rate) and the current commanded value for the selected mode. To the right of the ADI are three moving tape displays for horizontal speed (fps), altitude (ft) and altitude rate (fps).

The left display has a "moving map" with a pink triangle in the center representing the spacecraft; the red circle indicates the landing site. The rings indicate range from the spacecraft's current location, and the radial lines indicate bearing angles in increments of 30 deg. The map display rescales (zooms in) as the spacecraft approaches the landing site. The green diamonds on the map display indicate the body x- and y-axis components of the vehicle's speed. The green lines on the map display are error needles that provide guidance for the vehicle's longitudinal and lateral speeds using Eq. 14. This guidance is "fly to" which means that in the illustration of Fig. 5 the pilot should move the THC forward and right to drive the error needles to zero. At the bottom of the map display are digital readouts of range-to-go as well as its x (down-range) and y (cross-range) components. To the right of the map display are thrust indicators and color-coded gauges showing propellant mass available for the main descent engine and the RCS jets.
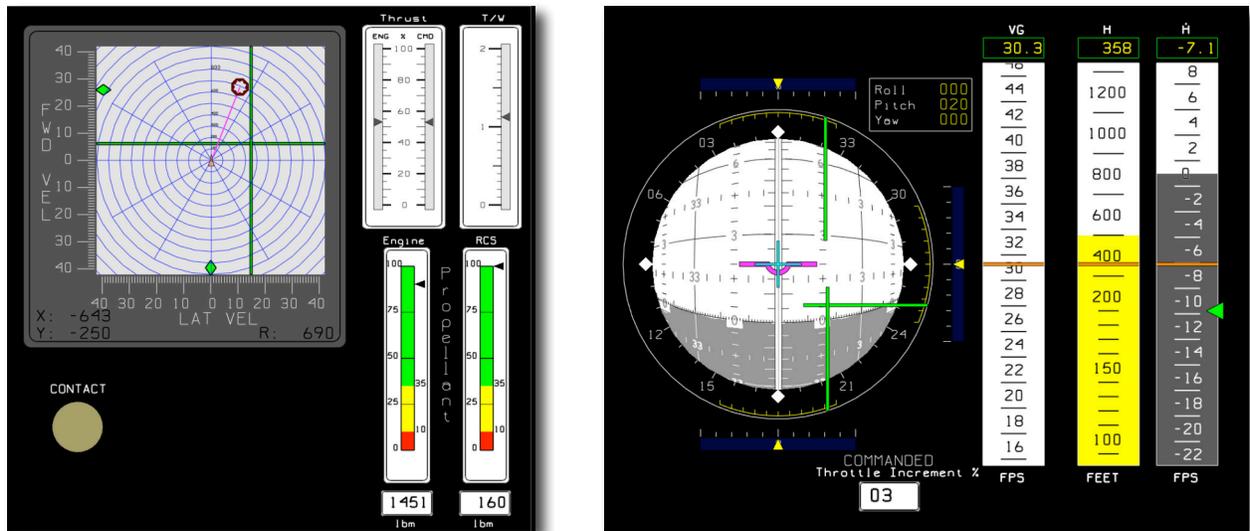
Figure 5. Pilot station displays

Results

This section provides a detailed analysis of the experiment data. There were a total of 180 data collection runs: 108 for the guidance-on configurations and 72 for the guidance-off configurations, as described below.

Guidance On

As described in a previous section, guidance laws were designed to follow the reference trajectory shown in Fig. 1. This reference trajectory was built using key parameters from the Apollo Lunar Module's descent profile. Pilots were advised to follow the roll/pitch angle guidance on the ADI using the RHC until the vehicle was in a near-level attitude, and then follow the forward/lateral velocity commands on the map display using the THC until touchdown. Strictly following the reference trajectory also requires following the rate-of-descent guidance commands from Eq. (11), but early testing indicated that this added substantially to the pilot workload. For the experiment, a simpler technique was used that approximated the descent rate profile of the reference trajectory. The simulation began in throttle increment mode with a ΔT_{cmd} setting of 3% that gradually reduced the descent rate from an initial value of 16 fps to roughly 3 fps when the vehicle was about 50 ft from the landing site. Pilots were advised to switch to rate-of-descent mode at this point, and if necessary adjust the descent rate to 3 fps.

Data were collected from six pilots for six values of control power ranging from 100% to 15% of the nominal value. The flying task was described in the section on experiment design; it is noted that there is a left offset of 250 ft at the initial condition. Pilots were generally able to follow the guidance commands without much difficulty. Figure 6 shows the actual trajectory profiles flown by the six pilots (three data runs each) for the 100% control power configuration. Note that all 18 trajectory profiles are orderly and bunched closely together.

American Institute of Aeronautics and Astronautics
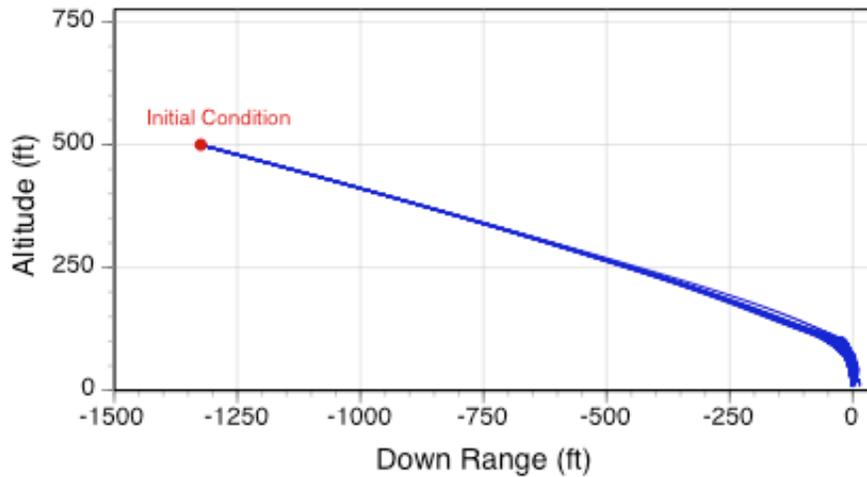
Figure 6. Longitudinal trajectory profiles for offset approach with guidance on, at 100% control power

Handling Qualities Ratings

Figure 7 shows the handling qualities ratings, on the Cooper-Harper scale, of all six pilots for each of the six control powers, i.e., 36 data points. In this bubble chart, the size of the bubble for a rating value indicates the number of pilots who assigned that rating. A star symbol indicates the median rating at each control power. For 100% control power the handling qualities ratings are essentially Level 1, and for 50% control power they straddle the Level 1 – 2 boundary. For 30% control power, the handling qualities ratings are essentially Level 2. For lower control powers (25% to 15%) the handling qualities ratings straddle the Level 2 – 3 boundary.
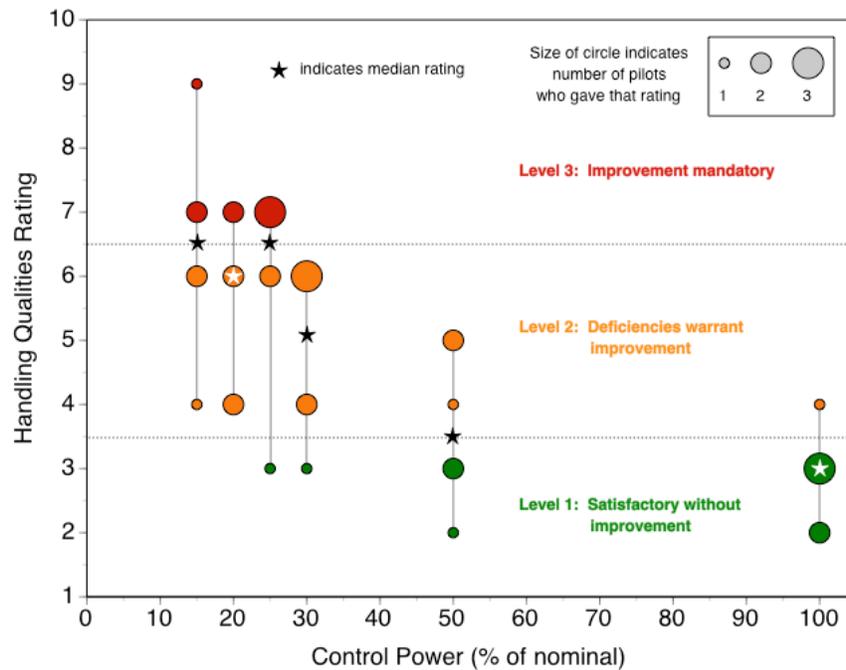
Figure 7. Handling qualities rating vs. control power, for offset approach with guidance on

American Institute of Aeronautics and Astronautics

The data in Fig. 7 exhibit some outliers that merit discussion. The rating of 9 at 15% control power was assigned because adequate performance could not be achieved (this requires a rating of 8 or worse). In the first two data runs, the range at touchdown was close to the limit of 15 ft; in the third run the range was 23 ft and the vehicle was almost out of descent engine propellant because there was a lot of back-and-forth maneuvering that almost doubled the nominal flying time. The ratings of 3 for the 25% and 30% control power configurations came from a pilot who consistently gave better ratings than the other five pilots. The rating of 4 for the 100% control power configuration came from a pilot who mostly gave worse ratings than the other five pilots.

Task Load Index Ratings

Figure 8 shows Task Load Index (TLX) ratings of all six pilots for each of the six control powers, i.e., 36 data points. Each data point, indicated by a blue dot in Fig. 8, was computed as the average of the individual TLX component ratings assigned by a pilot. It is noted that the component ratings were assigned by pilots on a scale of 1 to 10, and were converted to a scale of 0 to 100 in post-processing. A star symbol indicates the median rating at each control power. The horizontal line at a TLX value of 30 represents one interpretation of a workload requirement (upper limit) for tasks that could result in loss of mission.[20] The general trends of the TLX ratings are similar to those of the Cooper-Harper ratings. For 100% control power, the median TLX rating is around 25. At 50% control power, it lies close to the threshold value of 30. For lower control powers (30% to 15%) there is not much variation, and the median values are around 50. Recalling that the overall TLX rating is a composite of six individual components, it is noted that largest contribution to the TLX rating came from the effort component, and the lowest contribution came from the performance component.
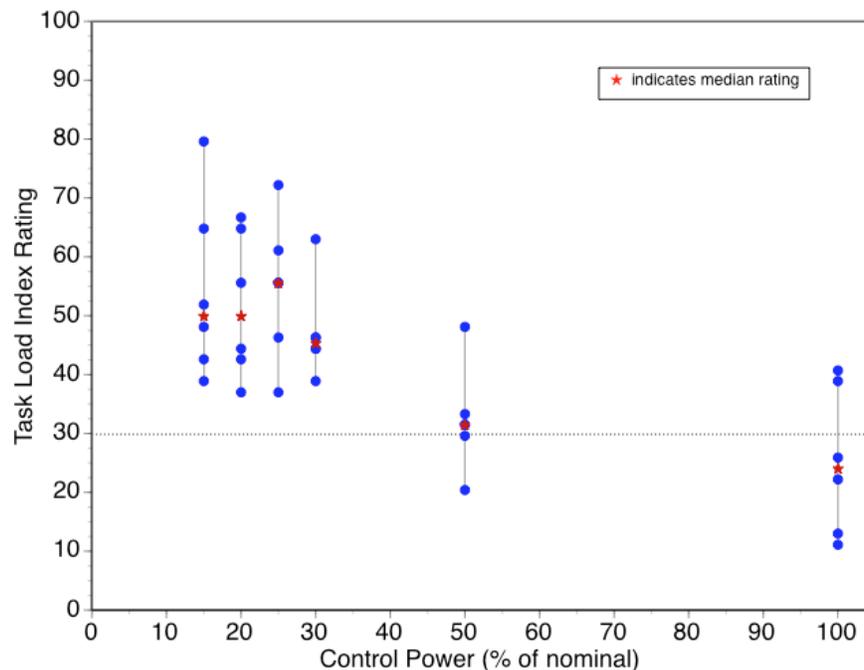
Figure 8. Task Load Index rating vs. control power, for offset approach with guidance on

Touchdown Performance

There were 10 parameters for touchdown performance; see Table 2 for a listing of these parameters and the corresponding limits for adequate performance. Data analysis revealed that adequate performance was generally achieved for all performance parameters. For example, Fig. 9 shows the dispersions of touchdown range (distance from center of landing pad) along with the limits of adequate performance shown by red circles, for 100% and 15% control powers. The 18 data points (blue dots) cover three runs for each of the six pilots. The median touchdown range for 100% control power was 1.7 ft (0.5 m) compared to 7.8 ft (2.4 m) for 15% control power, indicating that touchdown performance degrades as control power decreases.
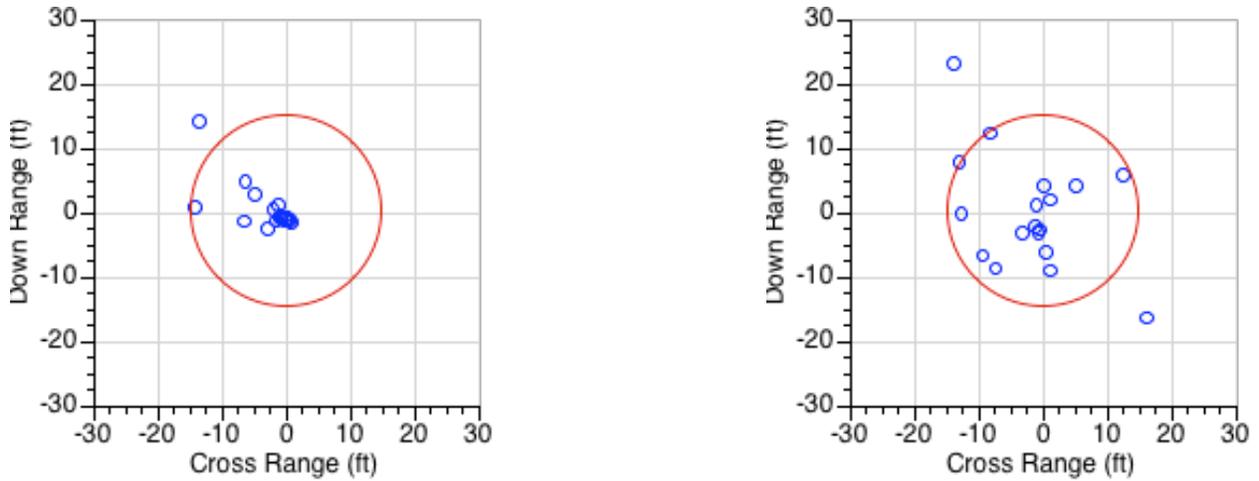
Figure 9. Touchdown range for 100% (left) and 15% (right) control powers, for offset approach with guidance on

Guidance Off

The original experiment plan was to evaluate handling qualities for the offset approach flying task across various control powers, with and without guidance. This would have permitted a direct comparison of handling qualities, at each control power, for guidance on vs. off. However, it was found that the offset approach precision landing task was extremely difficult to fly without guidance, even for pilots with significant flying skills and experience. Within the constraints of limited time available for training and familiarization, none of the pilots was able to develop a good technique to consistently fly the offset approach with guidance off. However, they were able to develop their own techniques to fly a centerline (zero lateral offset) approach with guidance off; the techniques often involved designing a series of "gates" at various altitudes and associating them with target values of horizontal speed.

Due to schedule and other constraints, experiment data with guidance off were collected from four of the six evaluation pilots. Data were collected from these pilots for six values of control power ranging from 100% to 15% of the nominal value. The flying task was described in the section on experiment design; it is noted that there is no lateral offset at the initial condition. Figure 10 shows the actual trajectory profiles flown by the four pilots (three data runs each) for the 100% control power configuration. Note that many of the 12 trajectory profiles are disorderly and show significant variations.
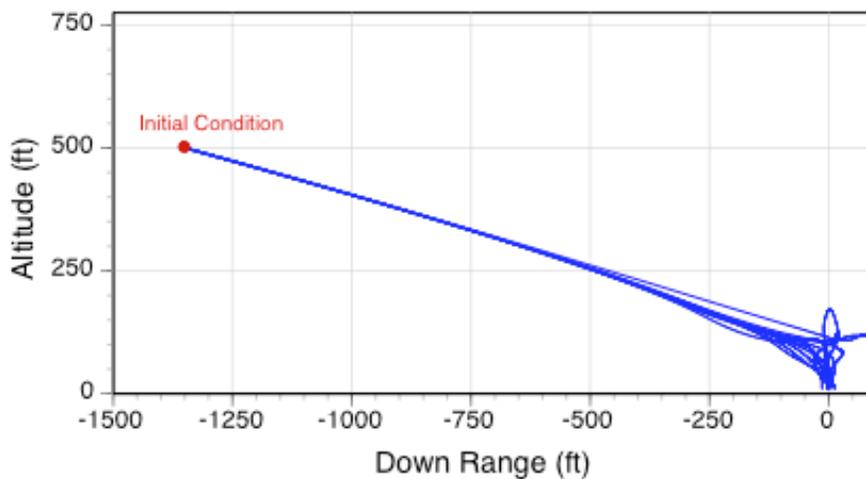
Figure 10. Longitudinal trajectory profiles for centerline approach with guidance off, at 100% control power

American Institute of Aeronautics and Astronautics

Results for the guidance off case are presented with an important caveat: they cannot be directly compared with corresponding configurations for guidance on because the flying tasks are different (offset approach with guidance on vs. centerline approach with guidance off). Even within the guidance-off configurations, the data variability across pilots may be significant since each pilot developed his own flying technique.

Handling Qualities Ratings

Figure 11 shows the handling qualities ratings, on the Cooper-Harper scale, of all four pilots for each of the six control powers, i.e., 24 data points. In this bubble chart, the size of the bubble for a rating value indicates the number of pilots who assigned that rating. A star symbol indicates the median rating at each control power. For 100% control power the handling qualities ratings are all Level 1, and for 50% control power they straddle the Level 1 – 2 boundary. For lower control powers (30% to 15%) the handling qualities ratings do not exhibit a clear trend. It is noted that there are no Level 3 ratings.
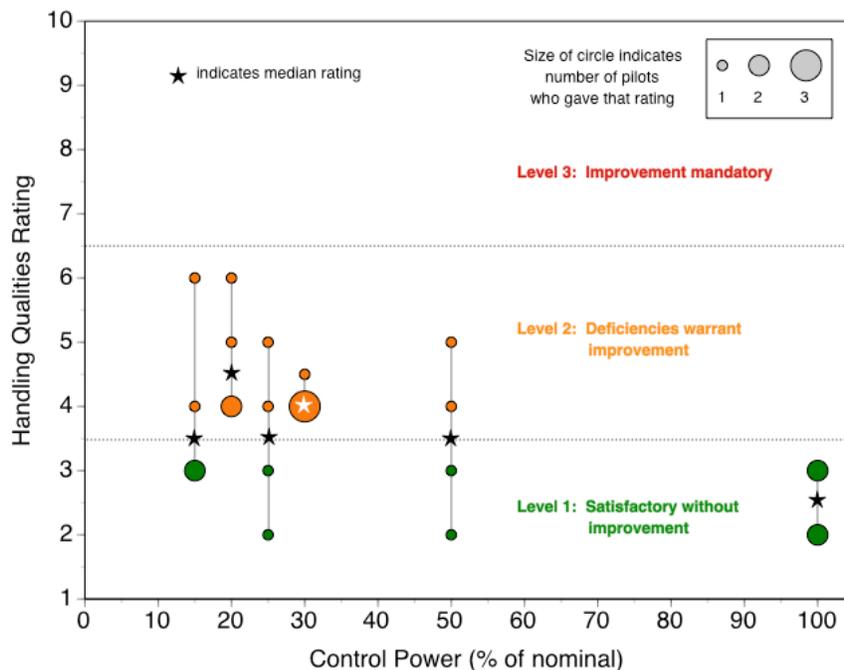
Figure 11. Handling qualities rating vs. control power, for centerline approach with guidance off

Task Load Index Ratings

Figure 12 shows Task Load Index (TLX) ratings of all four pilots for each of the six control powers, i.e., 24 data points. Each data point, indicated by a blue dot in Fig. 12, was computed as the average of the individual TLX component ratings assigned by a pilot. It is noted that the component ratings were assigned by pilots on a scale of 1 to 10, and were converted to a scale of 0 to 100 in post-processing. A star symbol indicates the median rating at each control power. The horizontal line at a TLX value of 30 represents one interpretation of a workload requirement (upper limit) for tasks that could result in loss of mission.[20] The general trends of the TLX ratings are similar to those of the Cooper-Harper ratings. For 100% control power, the median TLX rating is around 15. At 50% control power, it lies close to the threshold value of 30. For lower control powers (30% to 15%) the median values range from roughly 35 to 50. Recalling that the overall TLX rating is a composite of six individual components, it is noted that largest contribution to the TLX rating came from the effort component, and the lowest contribution came from the performance component.
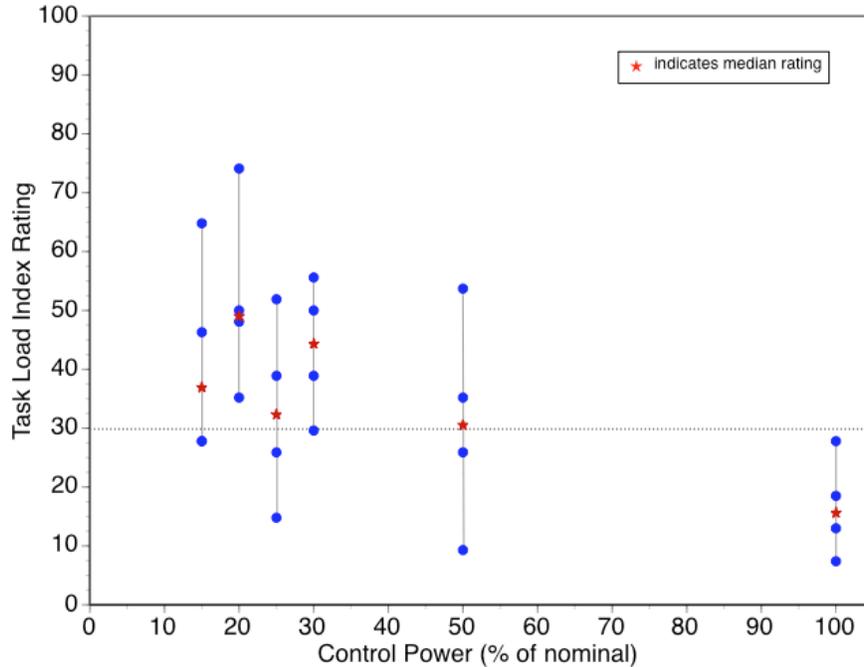
Figure 12. Task Load Index rating vs. control power, for centerline approach with guidance off

Touchdown Performance

There were 10 parameters for touchdown performance; see Table 2 for a listing of these parameters and the corresponding limits for adequate performance. Data analysis revealed that adequate performance was generally achieved for all performance parameters. For example, Fig. 13 shows the dispersions of touchdown range (distance from center of landing pad) along with the limits of adequate performance shown by red circles, for 100% and 15% control powers. The 12 data points (blue dots) cover three runs for each of the four pilots. The median touchdown range for 100% control power was 1.7 ft (0.5 m) compared to 6.2 ft (1.9 m) for 15% control power, indicating that touchdown performance degrades as control power decreases.
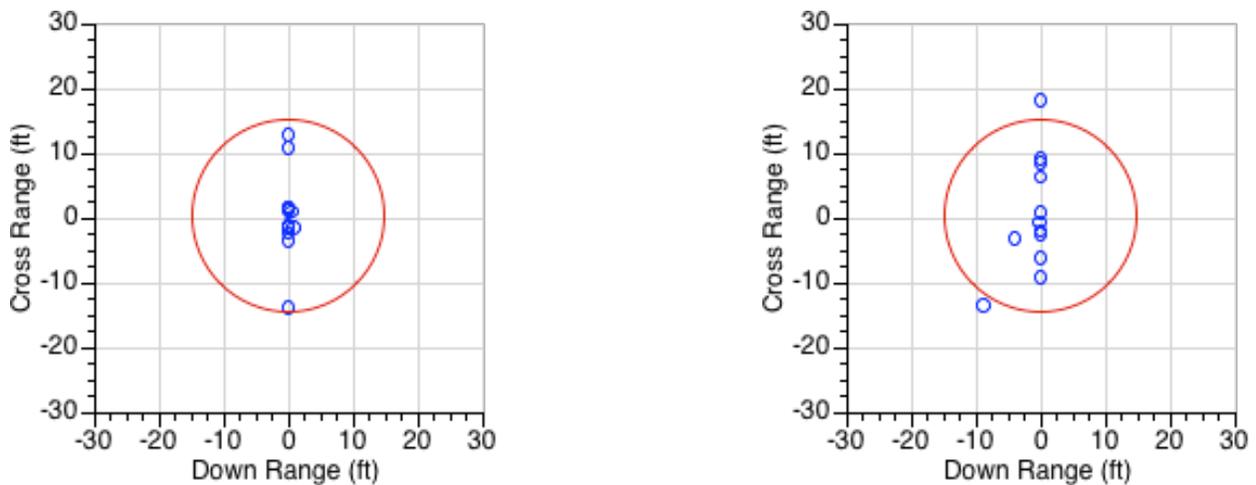
Figure 13. Touchdown range for 100% (left) and 15% (right) control powers, for centerline approach with guidance off

Conclusions

A piloted evaluation of lunar lander handling qualities was conducted by six pilot astronauts flying the NASA Ames Vertical Motion Simulator (VMS). The objective was to study the effects of control power and guidance cues on handling qualities for a precision landing task from terminal descent to touchdown.

For a lateral offset approach with guidance on, the handling qualities degraded nonlinearly as control power decreased. For 100% control power the handling qualities ratings were essentially Level 1, and for 50% control power they straddled the Level 1 – 2 boundary. For 30% control power the handling qualities ratings were essentially Level 2. For lower control powers (25% to 15%) the handling qualities ratings straddled the Level 2 – 3 boundary. The TLX ratings exhibited similar trends. Adequate performance was generally achieved for all performance parameters. For touchdown range, the median value for 100% control power was 1.7 ft compared to 7.8 ft for 15% control power, indicating that touchdown performance degrades as control power decreases.

The task of precision landing from offset approach was extremely difficult to fly without guidance, even for pilots with significant flying skills and experience. Within the constraints of limited time available for training and familiarization, none of the pilots was able to develop a good technique to consistently fly the offset approach with guidance off. However, they were able to develop their own techniques to fly a centerline (zero lateral offset) approach with guidance off; the techniques often involved designing a series of "gates" at various altitudes and associating them with target values of horizontal speed. For 100% control power, the handling qualities ratings were all Level 1, and for 50% control power they straddled the Level 1 – 2 boundary. For lower control powers (30% to 15%) there was no clear trend in handling qualities ratings, which were mainly in Level 2. The TLX ratings were qualitatively similar to the Cooper-Harper ratings. Adequate performance was generally achieved for all performance parameters. For touchdown range, the median value for 100% control power was 1.7 ft compared to 6.2 ft for 15% control power, indicating that touchdown performance degrades as control power decreases.

This initial experiment demonstrates that a precision landing requirement adds substantial difficulty to the already challenging flying task from terminal descent to lunar touchdown. The results clearly establish the need for good handling qualities in terms of control power requirements, as well as the need for appropriate guidance cues.

Acknowledgments

References

[1] Cooper, G.E. and Harper, R.P., "The Use of Pilot Rating in the Evaluation of Aircraft Handling Qualities," NASA TN D-5153, April 1969.

[2] Soule, H.A., "Preliminary Investigation of the Flying Qualities of Airplanes," NACA Report 700, 1940.

[3] Gilruth, R.R., "Requirements for Satisfactory Flying Qualities of Airplanes," NACA TR 755, 1943.

[4] Cooper, G.E. and Harper, R.P., "Handling Qualities and Pilot Evaluation," *Journal of Guidance, Control, and Dynamics*, Vol. 9, No. 5, Sep-Oct 1986, pp. 515-529.

[5] "Military Specification, Flying Qualities of Piloted Airplanes," MIL-F-8785C, Nov 1980.

[6] "Aeronautical Design Standard, Performance Specification: Handling Qualities Requirements for Military Rotorcraft," ADS-33, May 1996.

[7] Cheatham, D.C. and Hackler, C.T., "Handling Qualities for Pilot Control of Apollo Lunar-Landing Spacecraft," *Journal of Spacecraft*, Vol. 3, No. 5, May 1966, pp. 632-638.

[8] Hackler C.T., Brickel, J.R., Smith, H.E., and Cheatham, D.C., "Lunar Module Pilot Control Considerations," NASA TN D-4131, February 1968.

[9] Powers, B.G., "Space Shuttle Longitudinal Landing Flying Qualities," *Journal of Guidance, Control, and Dynamics*, Vol. 9, No. 5, Sep-Oct 1986, pp. 566-572.

[10] Jarvis, C.R., "Flight Test Evaluation of an On-Off Rate Command Attitude Control System of a Manned Lunar-Landing Research Vehicle," NASA TN D-3903, April 1967.

[11] "NASA's Exploration Systems Architecture Study," NASA TM-2005-214062, Nov 2005.

[12]Mueller, E.R., Bilimoria, K.D., and Frost, C.F., "Initial Handling Qualities Evaluation for Spacecraft Docking in Low Earth Orbit," Paper No. 2008-6832, *AIAA Guidance, Navigation, and Control Conference*, August 2008.

[13]Bailey, R.E., Jackson, E.B., and Goodrich, K.H., "Initial Investigation of Reaction Control System Design on Spacecraft Handling Qualities for Earth Orbit Docking," Paper No. 2008-6553, *AIAA Guidance, Navigation, and Control Conference*, August 2008.

"[14]Oral History Transcript," NASA Johnson Space Center Oral History Project, 19 September 2001, URL: www.nasa.gov/pdf/62281main_armstrong_oralhistory.pdf [cited 25 July 2008].

[15]Hart, S.G. and Staveland, L.E., "Development of NASA-TLX (Task Load Index): Results of Empirical and Theoretical Research," in *Human Mental Workload*, P.A. Hancock and N. Meshkati (Eds.), North Holland Press, Amsterdam, The Netherlands, 1988, pp. 239-350.

[16]Donahue, B.B., Caplin, G.N., and Smith, D.B., "Lunar Lander Concept Design for the 2019 NASA Outpost Mission," Paper No. 2007-6175, *AIAA Space 2007 Conference*, September 2007.

[17]Shelton, D.H., "Apollo Experience Report – Guidance and Control Systems: Lunar Module Stabilization and Control System," NASA TN D-8086, November 1975.

[18]Danek, G.L., "Vertical Motion Simulator Familiarization Guide," NASA TM 103923, May 1993.

[19]Aponso, B.L., Tran, D.T., and Schroeder, J.A. "Rotorcraft Research at the NASA Vertical Motion Simulator*," Proceedings of the 64th Annual Forum of the American Helicopter Society*, April 2008.

[20]"Human-Rating Requirements and Guidelines for Space Flight Systems," NASA Procedures and Guidelines, NPG 8705.2, June 2003.

American Institute of Aeronautics and Astronautics